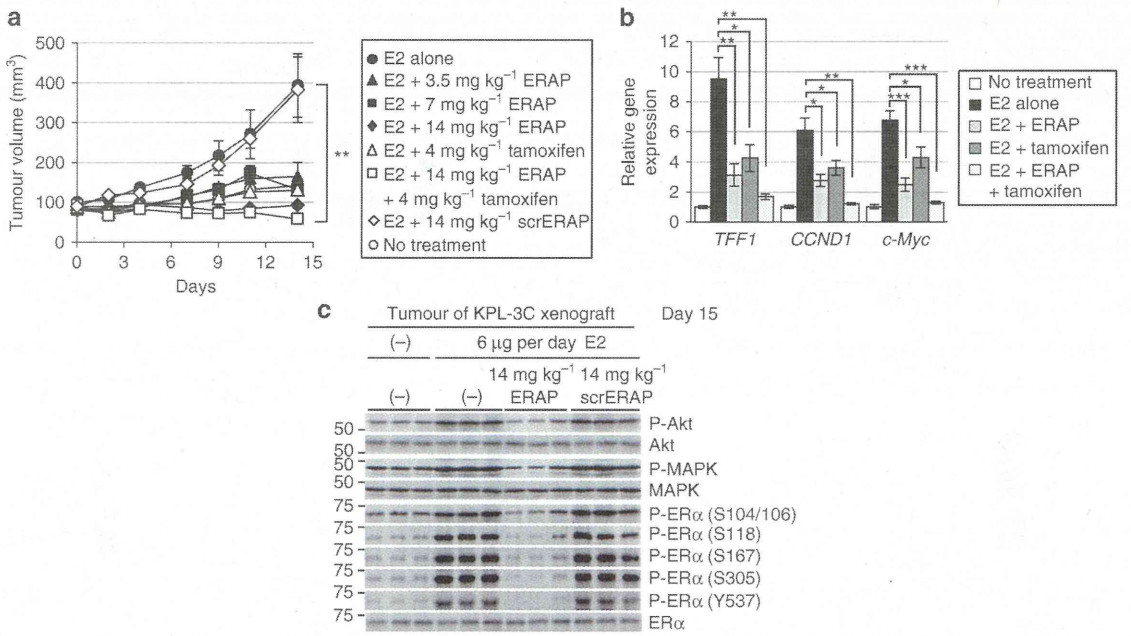

Figure 6 | ERAP inhibits tumour growth in xenograft models of human ERα-positive breast cancer. (**a**) ERAP inhibits tumour growth in a human breast cancer KPL-3C xenograft mouse model. The tumour volume represents the mean ± s.e.m. of each group ($n=5$; $^{**}P<0.01$ in two-sided Student's *t*-test). (**b**) Real-time PCR was performed to determine the combined inhibitory effects of ERAP and tamoxifen on the expression of ERα target genes. The data are expressed the fold increase over untreated cells at 0 h (set at 1.0) and represent the mean ± s.e.m. of each group ($n=5$; $^{*}P<0.05$, $^{**}P<0.01$, $^{***}P<0.001$ in two-sided Student's *t*-test). (**c**) Immunoblot analyses were performed to evaluate the effects of ERAP on the phosphorylation levels of Akt, p42/44 MAPK and ERα proteins in tumours.

xenografts in nude mice. Daily treatment with E2 alone induced time-dependent growth of KPL-3C and MCF-7 tumours, whereas treatment with 14 mg kg^{-1} ERAP caused significant inhibition of E2-induced tumour growth compared with mice treated with E2 alone or scrERAP in both tumour cell lines (14 mg kg^{-1}; $n=5$; $P<0.01$ in two-sided Student's *t*-test; Fig. 6a and Supplementary Fig. S6a). No toxicity or significant body weight changes were observed in either xenograft throughout these experiments (Supplementary Fig. S6b). As expected, a significant reduction in mRNA levels was evident for *TFF1*, *CCND1*, and *c-Myc* in tumours treated with ERAP compared with those treated with scrERAP or vehicle only (Fig. 6b and Supplementary Fig. S6c). Furthermore, considerable suppression of Akt, p42/44 MAPK and ERα phosphorylation was observed in tumours treated with ERAP (Fig. 6c and Supplementary Fig. S6d). More importantly, the combined treatment of ERAP and tamoxifen additively inhibited the expression of ERα target genes (Fig. 6b) and the development of KPL-3C xenografts as compared with tamoxifen or ERAP alone (Fig. 6a). These results demonstrated that ERAP had *in vivo* anti-tumour activity and could enhance the anti-tumour effects of tamoxifen.

ERAP suppresses growth of TAM-R tumours. To confirm that ERAP had an anti-tumour effect against endocrine-resistant breast cancer, we first examined the effects of ERAP on the activation of the non-genomic signalling pathway, on the phosphorylation of ERα and on the non-canonical ERα transcriptional activation via AP-1, which is responsible for tamoxifen resistance[10,11,16] in TAM-R MCF-7 (ref. 45) and T47D (ref. 46) cells. The phosphorylation levels of Akt, p42/44 MAPK and ERα were enhanced in response to tamoxifen alone or a combination of tamoxifen and E2, whereas ERAP treatment clearly suppressed these responses in both cell types (Fig. 7a,b and Supplementary Fig. S7a). ERAP treatment also clearly suppressed the phosphorylation levels of Akt, p42/44 MAPK and ERα in response to a combination of E2 and IGF-2 in the presence of tamoxifen in TAM-R T47D cells (Fig. 7b). In addition, ERAP significantly inhibited E2-induced ERα transcriptional activity via AP-1, as well as ERE (Supplementary Fig. S7b), and the E2-induced expression of *TFF1*, *CCND1* and c-*Myc* genes (Supplementary Fig. S7c,d) in the presence of tamoxifen in TAM-R MCF-7 or TAM-R T47D cells.

Next, we tested the ability of ERAP to inhibit the E2-dependent growth of TAM-R cells and found that ERAP treatment significantly reduced the growth of TAM-R MCF-7 (Fig. 7c) and TAM-R T47D cells (Fig. 7d) in the presence of tamoxifen. Furthermore, we examined the inhibitory effects of ERAP on the E2-dependent tumour growth of TAM-R MCF-7 and T47D orthotropic breast cancer xenografts in nude mice. The results demonstrated that E2-induced growth of both TAM-R tumours was suppressed by treatment with 14 mg kg^{-1} ERAP ($n=4$; $P<0.001$, Fig. 7e; $n=5$; $P<0.01$ in two-sided Student's *t*-test, Fig. 7f). Furthermore, considerable suppression of Akt, p42/44 MAPK and ERα phosphorylation was observed in both TAM-R tumours treated with ERAP (Supplementary Fig. S7e,f). Collectively, these data suggested that ERAP acted as an effective therapeutic agent with respect to endocrine-resistant breast cancer.

E2-dependent direct transactivation of *BIG3* by ERα. It was previously reported that *BIG3* is upregulated after E2 treatment in MCF-7 cells[21]. Thus, we hypothesized that *BIG3* may be a potential target gene of ERα and found that its expression was significantly upregulated in MCF-7 cells in a time-dependent manner after E2 stimulation (Fig. 8a). Interestingly, we also noted a significant reduction in *BIG3* expression at both the transcriptional and protein levels in a dose-dependent manner after tamoxifen treatment (Fig. 8b). Accordingly, to obtain direct

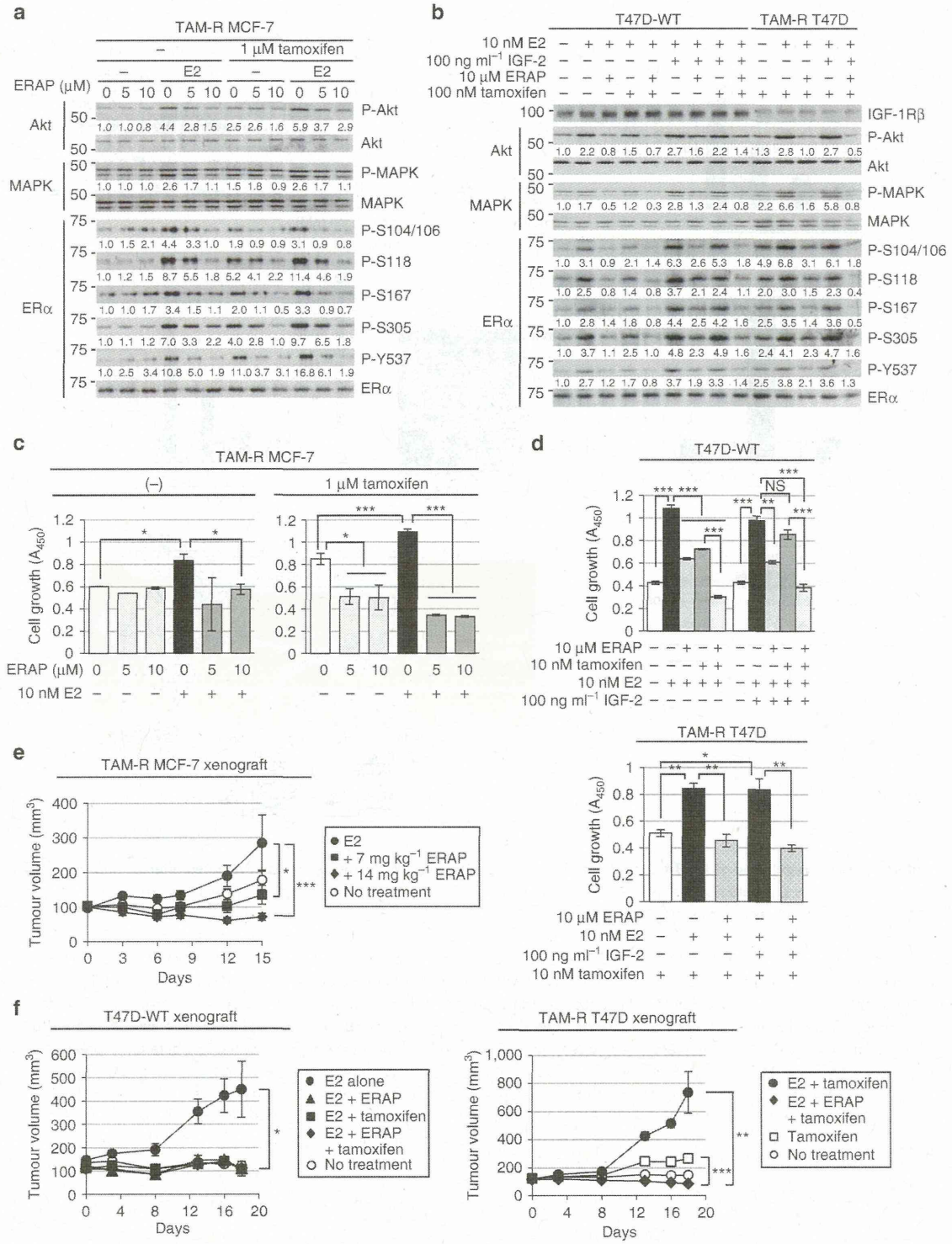

Figure 7 | ERAP suppresses growth of TAM-R tumours. (**a**,**b**) Immunoblot analyses were performed to evaluate the effects of ERAP on the phosphorylation levels of Akt, p42/44 MAPK and ERα proteins in TAM-R MCF-7 (**a**), and a parent T47D (T47D-WT) and TAM-R T47D (**b**) cells. (**c**) MTT (3-(4,5-dimethylthiazol-2-yl)-2,5-diphenyltetrazolium bromide) assays were performed to evaluate the inhibitory effect of ERAP on the growth of TAM-R MCF-7 cells. TAM-R MCF-7 cells were treated for 24 h with E2 ± ERAP in the presence or absence of 1 μM tamoxifen. The data represent the mean ± s.e.m. of three independent experiments (*$P<0.05$, ***$P<0.001$ in two-sided Student's *t*-test). (**d**) Inhibitory effect of ERAP on the growth of T47D-WT (upper) and TAM-R T47D (lower) cells after 24 h of treatment with E2 alone or E2 and IGF-2 in the presence and the absence of 10 nM tamoxifen, respectively. The data of all panels represent the mean ± s.e.m. of three independent experiments (*$P<0.05$, **$P<0.01$, ***$P<0.001$ in two-sided Student's *t*-test). (**e**) ERAP inhibits the tumour growth of TAM-R MCF-7 orthotropic breast cancer xenografts in nude mice. The tumour volume represents the mean ± s.e.m. of each group ($n=5$) (*$P<0.05$, ***$P<0.001$ in two-sided Student's *t*-test). (**f**) ERAP inhibits the tumour growth of both T47D-WT (left) and TAM-R T47D (right) orthotropic breast cancer xenografts in nude mice. The tumour volume represents the mean ± s.e.m. of each group ($n=5$; *$P<0.05$, **$P<0.01$, ***$P<0.001$ in two-sided Student's *t*-test).

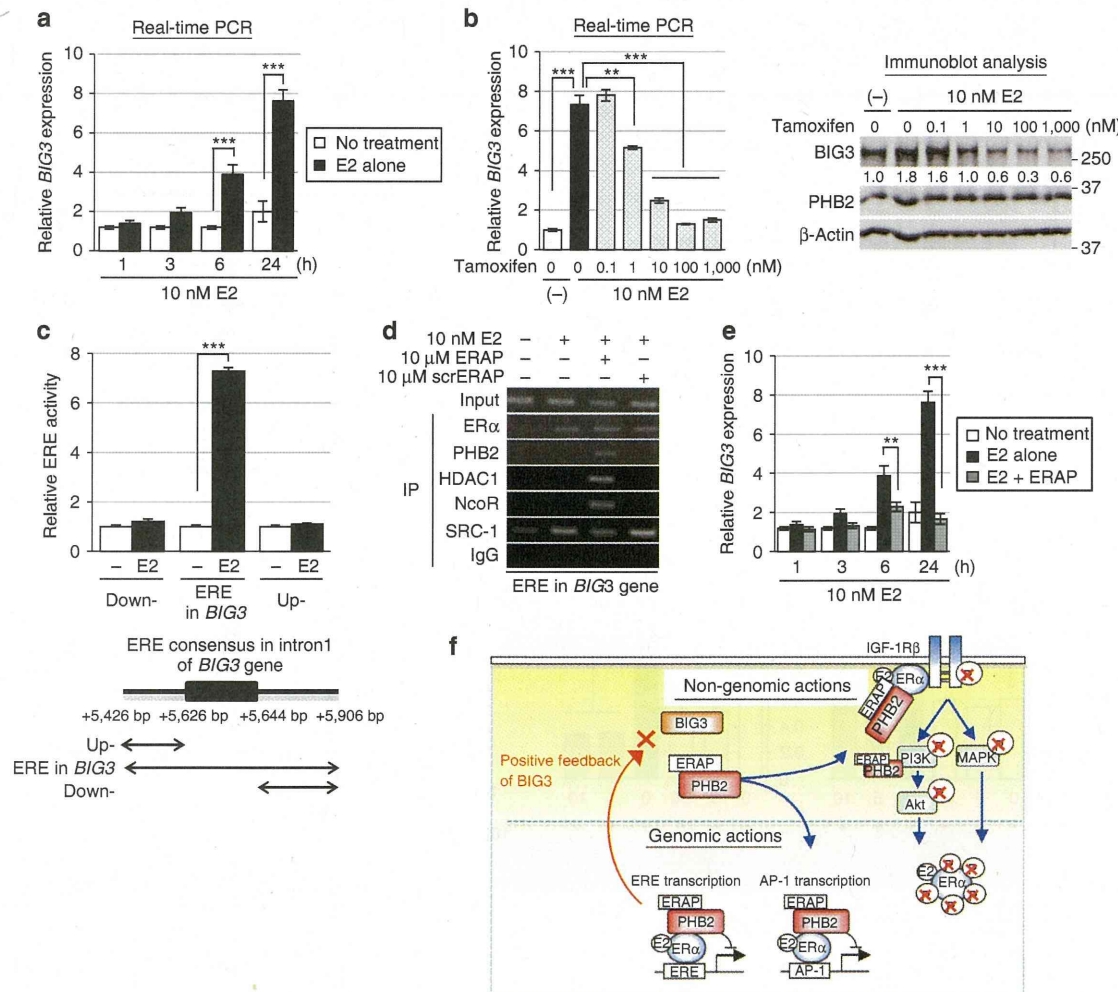

Figure 8 | Positive feedback regulation of *BIG3* transactivation. (**a**) Upregulation of *BIG3* expression was evaluated after E2 stimulation. These data are expressed the fold increase over untreated cells at 0 h (set at 1.0) and represent the mean ± s.e.m. of three independent experiments (***$P<0.001$ in two-sided Student's *t*-test). (**b**) The effects of tamoxifen were evaluated on *BIG3* expression. For real-time PCR analyses (left), the data are expressed as the fold increase over untreated cells (set at 1.0). These data represent the mean ± s.e.m. of three independent experiments (**$P<0.01$, ***$P<0.001$ in two-sided Student's *t*-test). For immunoblot analyses (right), β-actin served as a loading control. (**c**) Luciferase assays were performed to evaluate the transactivation of *BIG3* using a luciferase reporter containing an ERE motif conserved within intron 1 of the *BIG3* gene (5′-TCCAGTTGCATTGACCTGA-3′; 5,626–5,644 bp from the transcriptional start site of *BIG3*) or constructs containing the upstream and downstream regions lacking this ERE motif. The data represent the mean ± s.e.m. of three independent experiments (**$P<0.001$ in two-sided Student's *t*-test). (**d**) ChIP assays show the transactivation of *BIG3* through an intronic ERE. (**e**) The effect of ERAP on *BIG3* expression using real-time PCR is shown at the indicated time points. The data are expressed the fold increase over untreated cells at 0 h (set at 1.0) and represent the mean ± s.e.m. of three independent experiments (**$P<0.01$, ***$P<0.001$ in two-sided Student's *t*-test). (**f**) ERAP treatment leads to multiple levels of inhibition targeted at E2-dependent ERα activation pathways. ERAP competitively binds to endogenous PHB2, thereby preventing its interactions with BIG3. Free PHB2 directly binds to both nuclear and membrane-associated ERα, resulting in the repression of E2-induced ERα activation through non-genomic pathways and its phosphorylation. Moreover, ERAP also attenuates *BIG3* transcription, resulting in the downregulation of ERα target genes, including *BIG3*.

evidence for the upregulation of *BIG3* expression by ERα, we measured ERα transcriptional activity. E2 stimulation resulted in robust luciferase activity only in cells transfected with the construct containing an intronic ERE from *BIG3* (Fig. 8c), suggesting potential transactivation of *BIG3* by ERα. Next, we examined the recruitment of ERα to an intronic ERE motif of the *BIG3* gene by ChIP analysis (Fig. 8d). E2-dependent recruitment of ERα and the co-activator SRC-1 was observed associated with an ERE within intron 1 of the *BIG3* gene in MCF-7 cells. In contrast, ERAP treatment enhanced recruitment of HDAC1 and NcoR to the ERα–PHB2 complex (Fig. 8d). In addition, ERAP treatment led to significant suppression of the E2-induced expression levels of *BIG3* even after 3 h (Fig. 8e). These results demonstrated that *BIG3* was directly transactivated by ERα via its intronic ERE following E2 treatment, which suggested that *BIG3* acts through a positive feedback mechanism to enhance ERα activation in E2-dependent breast cancer cells. In other words, ERAP blocked this positive regulation of *BIG3*, leading to the release of PHB2 from cytoplasmic BIG3 and the inhibition of ERα activity via multiple mechanisms.

Discussion

In this study, we developed a dominant-negative peptide, ERAP, based on the residues Q165, D169 and Q173 in BIG3, which were essential for its heterodimerization with PHB2 to

suppress the growth of ERα-positive breast cancer cells, especially endocrine-resistant breast cancer cells. ERAP competitively bound endogenous PHB2, thereby preventing its interaction with BIG3 and releasing PHB2 to directly bind to both nuclear- and membrane-associated ERα. Intrinsic PHB2 binding to ERα led to the repression of a number of E2-induced activation events, which resulted in complete suppression of E2-dependent ERα-positive breast cancer cell growth *in vitro* and *in vivo* (Fig. 8f). These findings suggest that PHB2 has an important role in the modulation of multiple aspects of the E2/ERα-signalling network, although PHB2 has been reported to be the only transcriptional repressor for ERα. However, to date, it remains unclear how the endogenous tumour suppressor PHB2 is inactivated in cancer cells, despite abundant expression and the lack of genomic mutations or methylations in breast cancer clinical specimens or cell lines[47]. Our data suggest a potential solution to this unanswered problem; namely, our results suggest that BIG3 may sequester PHB2 in cancer cells, thereby causing an apparent 'loss-of-function' of PHB2 protein. These findings mark the first step toward uncovering a new E2/ERα signalling network in breast cancer and shed light on novel therapeutic strategies using PHB2 protein functions for E2/ERα-positive breast cancer.

The most important finding of this study was that ERAP might potentially act as an effective inhibitor of TAM-R breast cancer cells. Current endocrine therapies for breast cancer are based mainly on targeting the ERα-signalling pathway, and tamoxifen is the most frequently prescribed drug for the treatment of all stages of breast cancer[12,13]. However, tamoxifen resistance is a major clinical problem and a leading cause of treatment failure and mortality[14,15]. Compelling evidence suggests that multiply phosphorylated ERα and non-canonical ERα activation via AP-1 are linked to tamoxifen or aromatase inhibitor resistance in breast cancer cells[10,11,16]. In addition, the activation of the IGF-1Rβ/AKT–ERK1/2–MAPK network is also linked to tamoxifen resistance in breast cancers[10,11,16], even though the abundance of membrane-bound and cytoplasmic ERα is low in primary breast cancers[34]. Our study demonstrated that ERAP treatment completely inhibited ERα–IGF-1Rβ and/or ERα–PI3K interactions, ERα phosphorylation at multiple sites and ERα transcriptional activation via AP-1 in the presence of E2 in ERα-positive breast cancer cells. Indeed, ERAP had significant anti-tumour effects against TAM-R breast cancer cells. More importantly, we revealed that the combination of tamoxifen and ERAP induced rapid apoptosis and exhibited more potent anti-tumour activity *in vivo* and *in vitro* as compared with either treatment alone, indicating enhanced tamoxifen responsiveness. This combined effect is thought to be due to the distinct mechanisms of action of each drug, suggesting that releasing intrinsic PHB2 could suppress multifactorial mechanisms of endocrine resistance.

Current endocrine therapies, such as tamoxifen, pinpoint specific signalling pathways or molecules in the ERα-signalling network. In contrast, ERAP was shown to modulate multiple aspects of the E2/ERα-signalling network via the tumour suppressive ability of endogenous PHB2, which was expressed abundantly in cancer cells, leading to the complete suppression of E2-dependent breast cancer cell growth. Moreover, although *BIG3* is transactivated directly by ERα in a positive feedback loop, ERAP was shown to downregulate *BIG3* transcription, which reduced BIG3 protein levels in the cytoplasm of cancer cells and enabled endogenous PHB2 to suppress the extensive ERα signalling network. Moreover, as *BIG3* is specifically upregulated in breast cancer but is hardly detectable in normal human tissues, agents such as ERAP, which are designed to specifically disrupt BIG3 binding, may demonstrate excellent therapeutic indices with minimal off-target effects. Intracellular protein–protein interactions have been difficult to target with small molecules or synthetic peptide inhibitors, regardless of their ability to regulate many signalling networks. However, it has been reported that the Nutlins, selective small molecule antagonists of the MDM2–p53 interaction, possess *in vitro* and *in vivo* anti-tumour activity via the reactivation of p53 tumour suppressive activity[48]. In fact, as the inhibitory effect of ERAP was maintained for only 24 h (Supplementary Fig. S5b), it will be necessary to improve upon its pharmacologic properties using chemical synthetic approaches, such as hydrocarbon stapling methods[49,50], or to screen selective small molecule antagonists targeting the BIG3–PHB2 interaction.

In conclusion, targeting the BIG3–PHB2 interaction represents a potential new treatment avenue for ERα-positive breast cancer patients. This new approach could be an important supplement therapy and may provide mechanistic insight into the molecular basis of ERα-signalling networks in breast carcinogenesis. Thus, combining endocrine treatment with these new targeted therapies is a promising approach for improving the current treatment strategies and overcoming endocrine resistance, and should be investigated in future preclinical and clinical studies.

Methods

ERα antibody. The anti-ERα (clone AER314) antibody was purchased from Thermo Fisher Scientific (Fremont, CA). This antibody specifically recognizes undigested ERα and is equivalent to an anti-ERα antibody (SP-1)[34], which is widely used for immunohistochemical analysis (Supplementary Fig. S8).

Immunoblot analyses. Cells were lysed with lysis buffer (50 mM Tris-HCl, pH 8.0; 150 mM NaCl, 0.1% NP-40, 0.5% CHAPS) containing 0.1% protease inhibitor cocktail III (Calbiochem, San Diego, CA). The lysates were electrophoretically separated, blotted onto a nitrocellulose membrane and blocked with 4% BlockAce solution (Dainippon Pharmaceutical, Osaka, Japan) for 1 h. The blots were then incubated with antibodies against the following proteins: BIG3 (ref. 21) (1:200); PHB2 (1:500), NcoR (1:500) and ERα (phospho Y537; 1:500; Abcam, Cambridge, UK); SRC-1 (128E7; 1:500), Shc (1:500), α/β-tubulin (1:1,000), Akt (1:1,000), phospho-Akt (S473; 587F11; 1:1,000), p44/42 MAPK (1:500), phospho-p44/42 MAPK (T202/Y204; 1:500) and phospho-ERα (S104/S106; 1:500; Cell Signaling Technology, Danvers, MA); HDAC1 (H-11; 1:500), IGF-1Rβ (1:500), PI3-kinase p85α (U13; 1:500), phospho-ERα (S118; 1:500), phospho-ERα (S167; 1:500) and laminin B1 (1:100; Santa Cruz Biotechnology, Santa Cruz, CA); phospho-ERα (S305; 1:500; Millipore, Billerica, MA); phosphotyrosine (1:500; Zymed, San Francisco, CA); β-actin (AC-15; 1:5,000) and FLAG-tag M2 (1:5,000; Sigma, St Louis, MO); and HA-tag (1:3,000; Roche, Mannheim, Germany). After incubation with an horseradish peroxidase-conjugated secondary antibody (Santa Cruz Biotechnology, dilution 1:5,000) or monoclonal anti-rabbit immunoglobulins-peroxidase antibody (RG-16, Sigma, dilition 1:5,000) for 1 h, the blots were developed with an enhanced chemiluminescence system (GE Healthcare, Buckinghamshire, UK) and were scanned using an Image Reader LAS-3000 mini (Fujifilm, Tokyo, Japan). All experiments were performed more than three times in triplicate. Finally, the phosphorylation levels of IGF-1Rβ, Shc, PI3K, Akt, p42/44 MAPK and ERα were assessed through densitometric analysis of immunoblot results using an Image Reader LAS-3000 mini[51]. Full-length images of immunoblots are shown in Supplementary Fig. S9.

Immunoprecipitation. The cells were lysed with 0.1% NP-40 lysis buffer as described above. The cell lysates were precleared with normal IgG and rec-Protein G Sepharose 4B (Zymed) at 4 °C for 3 h. Then, the supernatants were incubated with antibodies against BIG3 (5 μg), PHB2 (5 μg) and ERα (5 μg) at 4 °C for 12 h. Next, the antigen–antibody complexes were precipitated with rec-Protein G Sepharose 4B at 4 °C for 1 h. Immunoprecipitated protein complexes were washed three times with lysis buffer and separated using SDS–PAGE. Immunoblot analyses were performed as described above.

Identification of the PHB2-binding regions in BIG3 protein. To determine the PHB2-binding region in BIG3, we cloned five different constructs corresponding to partial BIG3 sequences ($BIG3_{1-434}$, $BIG3_{435-2,177}$, $BIG3_{1,468-2,177}$, $BIG3_{1-100}$ and $BIG3_{1-250}$) into an amino-terminal FLAG-tagged pCAGGS vector. COS-7 cells were individually cotransfected with a BIG3 vector and HA-PHB2 using the FuGENE6 transfection reagent (Roche). At 48 h after transfection, the cells were lysed with 0.1% NP-40 lysis buffer. The lysates were precleared for 3 h at 4 °C and then incubated with anti-FLAG M2 agarose (Sigma) for 12 h at 4 °C. Next, the immunoprecipitated proteins or intact cell lysates were electrophoresed and blotted

onto nitrocellulose. Finally, the blots were incubated with antibodies against FLAG M2 or HA-tag.

Interaction site and structure prediction. BIG3 and PHB2 interaction sites were predicted using PSIVER. PSIVER is a computational method to predict residues that bind to other proteins using only sequence features (position-specific scoring matrix and predicted accessibility). The method uses the Naive Bayes classifier with kernel density estimation and was shown to outperform existing servers available on the Internet. The default threshold of 0.390 was used in this study. Structure prediction was performed using FUGUE[52] and PSIPRED[53]. A model of the putative PHB2-binding helix of BIG3 (residues 157–174) was built using MODELLER[54] based on the TIP120 protein[55] as a template.

BIG3–PHB2 interaction inhibition by ERAP. The 13 amino acid peptides derived from the PHB2-binding domain of BIG3 (codons 165–177) were covalently linked at the NH_2 terminus to a membrane transducing 11 polyarginine sequence (11R) to construct the ERAP peptide. Negative control peptides, scrERAP and mtERAP, were also synthesized. To examine the effects of ERAP on inhibition of BIG3–PHB2 complex formation, MCF-7 cells were treated with 10 nM E2 ± 10 μM ERAP. BIG3–PHB2 interactions were assessed using co-immunoprecipitation followed by immunoblotting, as described above.

Nuclear/cytoplasmic fractionation. MCF-7 cells were treated as described above, and nuclear and cytoplasmic/plasma membrane fractions were prepared using the NE-PER nuclear and cytoplasmic extraction reagent (Thermo Fisher Scientific) according to the manufacturer's instructions. α/β-Tubulin and laminin B were used as loading controls for the cytoplasmic and nuclear fractions, respectively.

Cell proliferation assay. Cell proliferation assays were performed using the Cell Counting Kit-8 (Dojindo, Kumamoto, Japan). The cells were plated in 48-well plates at 2×10^4 cells per well and maintained at 37 °C. At the indicated time points, a 1:10 dilution of the Cell Counting Kit-8 solution was added (into three replicate wells) and incubated for 1 h. Then, the absorbance at 450 nm was measured to calculate the number of vital cells per well. The data represent the mean ± s.e.m. of three independent experiments.

***In vivo* tumour growth inhibition.** Each suspension (1×10^7 cells per mouse) of KPL-3C cells, MCF-7 cells, T47D cells, TAM-R MCF-7 cells or TAM-R T47D cells was mixed with an equal volume of Matrigel (BD, Franklin Lakes, NJ) and injected (200 μl total) into the mammary fat pads of 6-week-old female BALB/c nude mice (Charles River Laboratories, Tokyo, Japan). The mice were housed in a pathogen-free isolation facility with a 12-h light/dark cycle, and were fed rodent chow and water *ad libitum*. The tumours developed over a period of 1 week, reaching sizes of ~100 mm^3 (calculated as $1/2 \times (\text{width} \times \text{length}^2)$). For KPL-3C orthotropic xenograft experiments, the mice were randomized into eight treatment groups (five animals per group): (1) no treatment; (2) 6 μg per day E2; (3–5) E2 + 3.5, 7 or 14 mg kg^{-1} per day ERAP; (6) E2 + 14 mg kg^{-1} per day scrERAP; (7) E2 + 4 mg kg^{-1} per day tamoxifen; and (8) E2 + 4 mg kg^{-1} per day tamoxifen + 14 mg kg^{-1} per day ERAP. For the MCF-7 orthotopic xenograft, the mice were randomized into three treatment groups: (1) 6 μg per day E2; (2) E2 + 14 mg kg^{-1} per day ERAP; and (3) E2 + 14 mg kg^{-1} per day scrERAP. For the T47D orthotopic xenograft, the mice were randomized into five treatment groups: (1) no treatment; (2) 6 μg per day E2; (3) E2 + 14 mg kg^{-1} per day ERAP; (4) E2 + 3.7 μg kg^{-1} per day tamoxifen; and (5) E2 + ERAP + tamoxifen. For TAM-R MCF-7 orthotropic xenograft, the mice were randomized into four treatment groups: (1) no treatment; (2) 37 μg kg^{-1} per day tamoxifen; (2) 6 μg per day E2 + tamoxifen; and (3, 4) E2 + tamoxifen + 7 or 14 mg kg^{-1} per day ERAP. For TAM-R T47D orthotopic xenografts, the mice were randomized into four treatment groups: (1) no treatment; (2) 3.7 μg kg^{-1} per day tamoxifen; (3) 6 μg per day E2 + tamoxifen; and (4) E2 + tamoxifen + 14 mg kg^{-1} per day ERAP. E2 was delivered via the application of a solution to the skin at the neck; the other treatments were delivered via intraperitoneal injection. Tumour volume was measured with calipers for 2 weeks, after which time the animals were killed, and the tumours were excised and frozen in liquid nitrogen. All experiments were performed in accordance with the guidelines of the animal facility at the University of Tokushima. For evaluations of the inhibitory effects of ERAP on tumour expression of ERα target genes using real-time PCR, the data are expressed as the fold increase in gene expression over the no treatment group (set at 1.0) and represent the mean ± s.e.m. of each group (five mice). In addition, for evaluations of the effects of ERAP on the phosphorylation of Akt, p42/44 MAPK and ERα proteins in tumours, each tumour lysates (three to four mice per group) was immunoblotted.

Statistical analyses. A Student's *t*-test was used to determine the significance of differences among the experimental groups. Values of $P < 0.05$ were considered significant.

The other methods are described in Supplementary Information.

References

1. McCracken, M. *et al.* Cancer incidence, mortality, and associated risk factors among Asian Americans of Chinese, Filipino, Vietnamese, Korean, and Japanese Ethnicities. *CA Cancer J. Clin.* **57,** 190–205 (2007).
2. Jemal, A. *et al.* Cancer statistics, 2006. *CA Cancer J. Clin.* **56,** 106–130 (2006).
3. Yager, J. D. & Davidson, N. E. Estrogen carcinogenesis in breast cancer. *N. Engl. J. Med.* **354,** 270–282 (2006).
4. Berry, D. A. *et al.* Effect of screening and adjuvant therapy on mortality from breast cancer. *N. Engl. J. Med.* **353,** 1784–1792 (2005).
5. Green, S. & Chambon, P. Nuclear receptors enhance our understanding of transcription regulation. *Trends Genet.* **4,** 309–314 (2000).
6. Kahlert, S. *et al.* Estrogen receptor rapidly activates the IGF-1 receptor pathway. *J. Biol. Chem.* **275,** 18447–18453 (2000).
7. Simoncini, T. *et al.* Interaction of oestrogen receptor with the regulatory subunit of phosphatidylinositol-3-OH kinase. *Nature* **407,** 538–541 (2000).
8. Castoria, G. *et al.* PI3-kinase in concert with Src promotes the S-phase entry of oestradiol-stimulated MCF-7 cells. *EMBO J.* **20,** 6050–6059 (2001).
9. Song, R. X. *et al.* The role of Shc and insulin-like growth factor 1 receptor in mediating the translocation of estrogen receptor α to the plasma membrane. *Proc. Natl Acad. Sci. USA* **101,** 2076–2081 (2004).
10. Osborne, C. K. & Schiff, R. Estrogen-receptor biology: continuing progress and therapeutic implications. *J. Clin. Oncol.* **23,** 1616–1622 (2005).
11. Johnston, S. R. New strategies in estrogen receptor-positive breast cancer. *Clin. Cancer Res.* **16,** 1979–1987 (2010).
12. Fisher, B. *et al.* Tamoxifen for prevention of breast cancer: report of the National Surgical Adjuvant Breast and Bowel Project P-1 Study. *J. Natl Cancer Inst.* **97,** 1652–1662 (2005).
13. Jordan, V. C. Tamoxifen: a most unlikely pioneering medicine. *Nat. Rev. Drug Discov.* **2,** 205–213 (2003).
14. Clarke, R., Leonessa, F., Welch, J. N. & Skaar, T. C. Cellular and molecular pharmacology of antiestrogen action and resistance. *Pharmacol. Rev.* **53,** 25–71 (2001).
15. Fisher, B., Dignam, J., Bryant, J. & Wolmark, N. Five versus more than five years of tamoxifen for lymph node-negative breast cancer: updated findings from the National Surgical Adjuvant Breast and Bowel Project B-14 randomized trial. *J. Natl Cancer Inst.* **93,** 684–690 (2001).
16. Ring, A. & Dowsett, M. Mechanisms of tamoxifen resistance. *Endocr. Relat. Cancer* **11,** 643–658 (2004).
17. Leary, A. F., Sirohi, B. & Johnston, S. R. Clinical trials update: endocrine and biological therapy combinations in the treatment of breast cancer. *Breast Cancer Res.* **9,** 112 (2007).
18. Leary, A. F. *et al.* Lapatinib restores hormone sensitivity with differential effects on estrogen receptor signaling in cell models of human epidermal growth factor receptor 2-negative breast cancer with acquired endocrine resistance. *Clin. Cancer Res.* **16,** 1486–1497 (2010).
19. Osborne, C. K. *et al.* Gefitinib or placebo in combination with tamoxifen in patients with hormone receptor-positive metastatic breast cancer: a randomized phase II study. *Clin. Cancer Res.* **17,** 1147–1159 (2011).
20. Nishidate, T. *et al.* Genome-wide gene-expression profiles of breast-cancer cells purified with laser microbeam microdissection: identification of genes associated with progression and metastasis. *Int. J. Oncol.* **25,** 797–819 (2004).
21. Kim, J. W. *et al.* Activation of an estrogen/estrogen receptor signaling by BIG3 through its inhibitory effect on nuclear transport of PHB2/REA in breast cancer. *Cancer Sci.* **100,** 1468–1478 (2009).
22. Montano, M. M. *et al.* An estrogen receptor-selective coregulator that potentiates the effectiveness of antiestrogens and represses the activity of estrogens. *Proc. Natl Acad. Sci. USA* **96,** 6947–6952 (1999).
23. Delage-Mourroux, R. *et al.* Analysis of estrogen receptor interaction with a repressor of estrogen receptor activity (REA) and the regulation of estrogen receptor transcriptional activity by REA. *J. Biol. Chem.* **275,** 35848–35856 (2000).
24. Murakami, Y. & Mizuguchi, K. Applying the naive bayes classifier with kernel density estimation to the prediction of protein-protein interaction sites. *Bioinformatics* **26,** 1841–1848 (2010).
25. Klinge, C. M. Estrogen receptor interaction with estrogen response elements. *Nucleic Acids Res.* **29,** 2905–2919 (2001).
26. Kushner, P. L. *et al.* Estrogen receptor pathways to AP-1. *J. Steroid Biochem. Mol. Biol.* **74,** 311–317 (2000).
27. Kurtev, V. *et al.* Transcriptional regulation by the repressor of estrogen receptor activity via recruitment of histone deacetylases. *J. Biol. Chem.* **279,** 24834–24843 (2004).
28. Varlakhabova, N., Snyder, C., Jose, S., Hahm, J. B. & Privalsky, M. L. Estrogen receptors recruit SMRT and N-CoR corepressors through newly recognized contacts between the corepressor N terminus and the receptor DNA binding domain. *Mol. Cell Biol.* **30,** 1434–1445 (2010).
29. Brown, A. M., Jeltsch, J. M., Roberts, M. & Chambon, P. Activation of pS2 gene transcription is a primary response to estrogen in the human breast cancer cell line MCF-7. *Proc. Natl Acad. Sci. USA* **81,** 6344–6348 (1984).

30. Altucci, L. *et al.* 17beta-Estradiol induces cyclin D1 gene transcription, p36D1-p34cdk4 complex activation and p105Rb phosphorylation during mitogenic stimulation of G (1)-arrested human breast cancer cells. *Oncogene* **12,** 2315–2324 (1996).
31. Dubik, D., Dembinski, T. C. & Shiu, R. P. Stimulation of c-myc oncogene expression associated with estrogen-induced proliferation of human breast cancer cells. *Cancer Res.* **47,** 6517–6521 (1987).
32. Jin, V. X., Rabinovich, A., Squazzo, S. L., Green, R. & Farnham, P. J. A computational genomics approach to identify cisregulatory modules from chromatin immunoprecipitation microarray data - a case study using E2F1. *Genome Res.* **16,** 1585–1595 (2006).
33. Yu, W. C., Leung, B. S. & Gao, Y. L. Effects of 17 beta-estradiol on progesterone receptors and the uptake of thymidine in human breast cancer cell line CAMA-1. *Cancer Res.* **41,** 5004–5009 (1981).
34. Welsh, A. W. *et al.* Cytoplasmic estrogen receptor in breast cancer. Clin. *Cancer Res.* **18,** 118–126 (2012).
35. Mintz, P. J. *et al.* The phosphorylated membrane estrogen receptor and cytoplasmic signaling and apoptosis proteins in human breast cancer. *Cancer* **113,** 1489–1495 (2008).
36. Murphy, L. C., Seekallu, S. V. & Watson, P. H. Clinical significance of estrogen receptor phosphorylation. *Endocr. Relat. Cancer* **18,** R1–R14 (2011).
37. Lannigan, D. A. Estrogen receptor phosphorylation. *Steroids* **68,** 1–9 (2008).
38. Chen, D. *et al.* Activation of estrogen receptor alpha by S118 phosphorylation involves a ligand-dependent interaction with TFIIH and participation of CDK7. *Mol. Cell* **6,** 127–137 (2000).
39. Chen, D., Pace, P. E., Coombes, R. C. & Ali, S. Phosphorylation of human estrogen receptor alpha by protein kinase A regulates dimerization. *Mol. Cell Biol.* **19,** 1002–1015 (1999).
40. Joel, P. B. *et al.* pp90rsk1 regulates estrogen receptor-mediated transcription through phosphorylation of Ser-167. *Mol. Cell Biol.* **18,** 1978–1984 (1998).
41. Rogatsky, I., Trowbridge, J. M. & Garabedian, M. J. Potentiation of human estrogen receptor alpha transcriptional activation through phosphorylation of serines 104 and 106 by the cyclin A-CDK2 complex. *J. Biol. Chem.* **274,** 22296–22302 (1999).
42. Arnold, S. F., Melamed, M., Vorojeikina, D. P., Notides, A. C. & Sasson, S. Estradiol-binding mechanism and binding capacity of the human estrogen receptor is regulated by tyrosine phosphorylation. *Mol. Endocrinol.* **11,** 48–53 (1997).
43. Wang, R. A., Mazumdar, A., Vadlamudi, R. K. & Kumar, R. P21-activated kinase-1 phosphorylates and transactivates estrogen receptor-alpha and promotes hyperplasia in mammary epithelium. *EMBO J.* **21,** 5437–5447 (2001).
44. Taylor, I. W., Hodson, P., Green, M. D. & Sutherland, R. L. Effects of tamoxifen on cell cycle progression of synchronous MCF-7 human mammary carcinoma cells. *Cancer Res.* **43,** 4007–4010 (1983).
45. Oyama, M. *et al.* Integrated quantitative analysis of the phosphoproteome and transcriptome in tamoxifen-resistant breast cancer. *J. Biol. Chem.* **286,** 818–829 (2011).
46. Fagan, D. H., Uselman, R. R., Sachdev, D. & Yee, D. Acquired resistance to tamoxifen is associated with loss of the type I insulin-like growth factor receptor: implications for breast cancer treatment. *Cancer Res.* **72,** 3372–3380 (2012).
47. Sato, T. *et al.* The human prohibitin (PHB) gene family and its somatic mutations in human tumours. *Genomics* **17,** 762–764 (1993).
48. Vassilev, L. T. *et al.* In vivo activation of the p53 pathway by small-molecule antagonists of MDM2. *Science* **303,** 844–848 (2004).
49. Walensky, L. D. *et al.* Activation of apoptosis in vivo by a hydrocarbon-stapled BH3 helix. *Science* **305,** 1466–1470 (2004).
50. Moellering, R. E. *et al.* Direct inhibition of the NOTCH transcription factor complex. *Nature* **462,** 182–188 (2009).
51. Abramoff, M. D., Magelhaes, P. J. & Ram, S. J. Image processing with Image J. *Biophotonics Int.* **11,** 36–42 (2004).
52. Shi, J., Blundell, T. L. & Mizuguchi, K. FUGUE: sequence-structure homology recognition using environment-specific substitution tables and structure-dependent gap penalties. *J. Mol. Biol.* **310,** 243–257 (2001).
53. McGuffin, L. J., Bryson, K. & Jones, D. T. The PSIPRED protein structure prediction server. *Bioinformatics* **16,** 404–405 (2000).
54. Eswar, N., Eramian, D., Webb, B., Shen, M. Y. & Sali, A. Protein structure modeling with MODELLER. *Methods Mol. Biol.* **426,** 145–159 (2008).
55. Goldenberg, S. J. *et al.* Structure of the Cand1-Cul1-Roc1 complex reveals regulatory mechanisms for the assembly of the multisubunit cullin-dependent ubiquitin ligases. *Cell* **119,** 517–528 (2004).

Acknowledgements

We thank Drs Douglas Yee and Dedra Fagan (University of Minnesota) for the gift of the TAM-R T47D cell line; Dr Takao Yamori (Cancer Chemotherapy Centre, Japanese Foundation for Cancer Research) for the gift of the HBC4 breast cancer cell line; Dr Junichi Kurebayashi (Kawasaki Medical School) for the gifts of the KPL-3C and KPL-1 breast cancer cell lines; Drs Kazuhiro Ikeda and Satoshi Inoue (Saitama Medical University) for the gifts of the TAM-R-MCF-7 cells; and Drs Tomoya Fukawa and Kazuma Kiyotani (The University of Tokushima) for helpful discussions. We acknowledge support from the Takeda Science Foundation, Naito Foundation, the Mochida Memorial Foundation for Medical and Pharmaceutical Research, the Takamatsunomiya Princess Memorial Foundation, Project Future of Relay For Life Japan and a Grant-in-Aid for Scientific Research on Innovative Areas from MEXT (T.K., 2011–2012) (23134504), (T.K., 2013-2014)(25134712).

Author contributions

T.Y. performed all experiments. M.K. performed *in vivo* experiments. T.M. performed the affinity purification of BIG3 antibody and was involved in functional analysis. Y.-A.C., Y.M. and K.M. performed *in silico* analysis for prediction of BIG3–PHB2 interaction. E.M. and T.I. performed purification of recombinant PHB2 protein. M.A. identified BIG3 through the expression profiling analysis. R.Y., S.I., S.M. and Y.M. discussed the interpretation of ER-signalling pathway data. M.S. collected breast cancer specimens. Y.N. supported the preparation of the final version of the manuscript. T.K. was involved in the conception and design of all studies, interpretation of data and preparing the draft and final version of the manuscript. All authors read and approved the final manuscript. M.K. and T.M. contributed equally to this work.

Additional information

Supplementary Information accompanies this paper at http://www.nature.com/naturecommunications

Competing financial interests: Toyomasa Katagiri is an external board member of OncoTherapy Science, Inc. The remaining authors declare no competing financial interest.

Reprints and permission information is available online at http://npg.nature.com/reprintsandpermissions/

How to cite this article: Yoshimaru, T. *et al.* Targeting BIG3–PHB2 interaction to overcome tamoxifen resistance in breast cancer cells. *Nat. Commun.* 4:2443 doi: 10.1038/ncomms3443 (2013).

Int J Clin Oncol
DOI 10.1007/s10147-013-0585-y

ORIGINAL ARTICLE

Influence of body mass index on clinicopathological factors including estrogen receptor, progesterone receptor, and Ki67 expression levels in breast cancers

Ayako Yanai · Yoshimasa Miyagawa · Keiko Murase · Michiko Imamura · Tomoko Yagi · Shigetoshi Ichii · Yuichi Takatsuka · Takashi Ito · Seiichi Hirota · Mitsunori Sasa · Toyomasa Katagiri · Yasuo Miyoshi

Received: 8 March 2013 / Accepted: 30 May 2013

Abstract
Background High body mass index (BMI) is associated not only with a higher incidence of breast cancers but also with poorer prognosis. It is speculated that both enhanced production of estrogens and other factors associated with obesity are involved in these associations, but the biological characteristics associated with high BMI have yet to be thoroughly identified.
Methods We studied 525 breast cancers, focusing on biological differences between tumors associated with high and low BMI and by immunohistochemically defined intrinsic subtype. Ki67 expression levels were used to differentiate luminal A from luminal B estrogen receptor (ER)+/human epidermal growth factor receptor 2 (HER2)- breast cancers.
Results Premenopausal patients with high BMI showed a significantly higher frequency of lymph node metastasis (46.4 % vs. 22.9 %, $P = 0.005$) and tended to have a larger tumor size ($P = 0.05$) and higher nuclear grade ($P = 0.07$) than those with low BMI. These differences were not observed among postmenopausal patients. BMI was not associated with distribution of breast cancer subtypes, and ER, progesterone receptor (PR), and Ki67 expression levels of each subtype showed no differences between high and low BMI among premenopausal patients.
Conclusion Higher BMI might influence aggressive tumor characteristics among premenopausal patients, but its influence on ER, PR, and Ki67 expression levels seems to be limited.

Keywords Body mass index · Breast cancer · Estrogen receptor · Ki67

A. Yanai · Y. Miyagawa · K. Murase · M. Imamura · T. Yagi · S. Ichii · Y. Takatsuka · Y. Miyoshi (✉)
Division of Breast and Endocrine, Department of Surgery, Hyogo College of Medicine, Mukogawa-cho 1-1, Nishinomiya, Hyogo 663-8501, Japan
e-mail: ymiyoshi@hyo-med.ac.jp

T. Ito · S. Hirota
Surgical Pathology, Hyogo College of Medicine, Mukogawa-cho 1-1, Nishinomiya, Hyogo 663-8501, Japan

M. Sasa
Tokushima Breast Care Clinic, Nakashimada-cho 4-7-7, Tokushima, Tokushima 770-0052, Japan

T. Katagiri
Division of Genome Medicine, Institute of Genome Research, Tokushima University, Kuramoto-cho 3-18-15, Tokushima, Tokushima 770-8503, Japan

Introduction

Body mass index (BMI) has been firmly established as being related to not only the incidence but also the prognosis of breast cancer. Because an increase in BMI is positively associated with breast cancer risk for postmenopausal patients but not premenopausal patients [1, 2], such an increase seems to be involved in breast cancer incidence, possibly through enhanced production of circulating estrogens [3]. This hypothesis seems to be supported by a reportedly positive association between BMI and ER-positive breast cancer risk for postmenopausal women [4]. It has further been reported that elevated BMI is significantly associated with worse prognosis, especially for pre-/perimenopausal patients [5]. Consistent with this finding, Kawai et al. [6] found that higher BMI was associated with an increase in mortality for premenopausal patients. Their analysis of subsets showed a positive association between

Published online: 03 July 2013

higher BMI and worse prognosis for patients with hormonal receptor (HR)-positive tumors. In addition, enhanced BMI in their study correlated with worse prognosis only for HR-positive and for human epidermal growth factor receptor 2 (HER2)-negative but not HER2-positive or triple-negative tumors, irrespective of menopausal status [7, 8].

Thus, the effect of BMI on breast cancer incidence and prognosis seems to be restricted to ER-positive breast cancers. However, it is not yet clear why prognosis correlates with BMI of premenopausal patients. In a study by Berclaz et al. [5], a positive association between BMI and prognosis was recognized for patients treated with chemotherapy but not with endocrine therapy. Similar findings were obtained in a study reported by Sparano et al. [7] in which adjuvant chemotherapy was administered to all patients. Furthermore, according to data from the ATAC (anastrozole, tamoxifen, alone, or in combination) trial, postmenopausal women with high BMI treated with anastrozole showed significantly more distant recurrences than those with a low BMI, possibly caused by ineffective suppression of estrogen production resulting from an increase in aromatase activity in patients with high BMI [9]. Nevertheless, in spite of these findings, it is currently still unknown how adjuvant treatments including chemotherapy and endocrine therapy affect the relationship between BMI and prognosis.

If the occurrence of tumors in patients with high BMI is the result of an increase in estrogen status, these tumors are likely to be highly estrogen dependent, thus resulting in a favorable prognosis. On the other hand, a poorer prognosis for patients with high BMI may indicate that BMI plays a significant part in breast cancer etiology and prognosis by mediation through various mechanisms. To determine the crucial role of BMI, the relationship between tumor biological characteristics and BMI of patients thus needs to be thoroughly analyzed, but this issue has not yet been specifically discussed in the literature. The purpose of the study presented here was to disclose the relationship between BMI at the time of diagnosis and biological characteristics, focusing specifically on ER, PR, and Ki67 expression levels in terms of different subtypes.

Materials and methods

Patients

The 525 cases of invasive breast cancers treated with mastectomy or breast-conserving surgery at Hyogo College of Medicine or Tokushima Breast Clinic between 2005 and 2012 were recruited consecutively. Histological diagnosis of breast cancer was confirmed in each case (493 invasive ductal carcinomas, 15 invasive lobular carcinomas, and 19 other types), and patients with noninvasive carcinoma were excluded. This study was approved by the Ethics Committee of Hyogo College of Medicine.

Immunohistochemical staining and classification of subtypes

For classification of subtypes, immunohistochemical staining of ER, PR, HER2, and Ki67 was performed. Formalin-fixed, paraffin-embedded tissues were cut and used for immunohistochemical analyses. Staining was followed by automated immunostaining with BOND-MAX (Leica Microsystems, Tokyo, Japan) for ER and PR, and with Autostainer (Dako, Tokyo, Japan) for HER2 and Ki67. The primary antibodies used for this study were ER (1D5), PR (PgR636), HER2 (Hercep Test), and Ki67 (MIB1), all from Dako (Glostrup, Denmark). Expression levels of these proteins were determined immunohistochemically as the percentage of positive cancer cells in the nuclei for ER, PR, and Ki67, and by membrane staining for HER2. When nuclear stained cells accounted for 1 % or more, they were deemed positive for ER and PR, and HER2 positivity was defined as HER2 (3+), or HER2 (2+) and fluorescence in situ hybridization (FISH) positive. Different areas of densely stained lesions were selected microscopically, and more than 500 cancer cells were counted to determine Ki67 expression levels.

The criteria reported by Cheang et al. [10] were used to separate ER-positive and HER2-negative breast cancers into luminal A and luminal B subtypes by using a cutoff point of 14 % Ki67. The subtypes were defined as follows: luminal A, ER+/HER2−, Ki67 < 14 %; luminal B, ER+/HER2−, Ki67 ≥ 14 %; luminal/HER2, ER+/HER2+; HER2, ER−/HER2+; and triple negative (TN), ER−/HER2−.

Statistical analysis

The relationship between BMI, calculated as weight (kg) divided by height (m^2), and breast cancer characteristics was determined with the chi squared test. ER, PR, and Ki67 expression levels for each subtype were calculated with the Mann–Whitney test. Differences were considered statistically significant if the P value was less than 0.05. JMP10 (SAS Institute Japan, Tokyo, Japan) was used for all analyses.

Results

Correlation between BMI and clinicopathological characteristics of breast cancers

The BMI of the postmenopausal patients (mean, 23.3 kg/m^2; standard deviation, 3.8 kg/m^2) was significantly higher than

that of premenopausal patients (22.0, 4.1) ($P < 0.0001$; Table 1). We used the categorization by Kawai et al. [6] of BMI of Japanese breast cancer patients into quartiles (<21.2, ≥21.2 to <23.3, ≥23.3 to <25.8, and ≥25.8 kg/m^2) to set 23.3 kg/m^2 as the median cutoff and divide the patients into high- and low-BMI level groups (low, <23.3 kg/m^2; high, ≥23.3 kg/m^2). As shown in Table 1, there were significantly more postmenopausal ($n = 153$, 73.9 %) than premenopausal patients with high BMI ($n = 56$, 26.1 %) ($P = 0.0002$; Table 1).

Table 2 shows that a significantly higher percentage of premenopausal than postmenopausal patients with high BMI had lymph node metastases (46.4 % vs. 22.9 %, $P = 0.005$), whereas the correlation between large tumor size (37.0 % vs. 23.7 %) and high nuclear grade (grade 3, 39.0 vs. grade 1, 27.8 %) was marginally significant ($P = 0.05$ and $P = 0.07$, respectively). However, the two groups of postmenopausal patients showed no significant differences in tumor size, nuclear grade, or histological type (Table 3). More postmenopausal patients with high BMI tended to have PR-positive than PR-negative tumors (48.9 % vs. 37.8 %, $P = 0.05$), but there was no significant difference in HER2 positivity between the two BMI groups.

Correlation between BMI and breast cancer subtypes

We also divided breast cancers into five groups: luminal A (ER+/HER2− and Ki67 < 14 %, $n = 237$), luminal B (ER+/HER2− and Ki67 ≥ 14 %, $n = 150$), luminal/HER2 (ER+/HER2+, $n = 40$), HER2-positive (ER−/HER2+, $n = 37$), and TN (ER−/HER2−, $n = 61$). There were no statistically significant differences between BMI and breast cancer subtypes (Table 4) even when menopausal status was factored in.

Table 1 Relationship between body mass index (BMI) and menopausal status of breast cancer patients

	n	Premenopausal	n	Postmenopausal	P value
Age[a] (years) (SD)	187	44.5 (6.5)	338	65.2 (9.8)	
BMI[a] kg/m^2 (SD)	187	22.0 (4.1)	338	23.3 (3.8)	<0.0001
BMI[b]	Premenopausal		Postmenopausal		P value
Low	133 (41.8 %)		185 (58.2 %)		0.0002
High	54 (26.1 %)		153 (73.9 %)		

[a] Mean (standard deviation)

[b] BMI: low, <23.3 kg/m^2; high, ≥23.3 kg/m^2

Table 2 Relationship between body mass index (BMI) and clinicopathological characteristics in premenopausal patients

Characteristics	Low BMI[a] (%)	High BMI[a] (%)	P value
Tumor size			
≤2.0 cm	87 (76.3)	27 (23.7)	0.05
<2.0 cm	46 (63.0)	27 (37.0)	
Lymph node metastasis			
Negative	101 (77.1)	30 (22.9)	0.005
Positive	32 (57.1)	26 (42.9)	
Nuclear grade			
1	83 (72.2)	32 (27.8)	0.07
2	21 (87.5)	3 (12.5)	
3	25 (61.0)	16 (39.0)	
Unknown	4 (44.4)	5 (55.6)	
Histological type[b]			
IDC	124 (71.7)	49 (28.3)	0.82
ILC	5 (62.5)	3 (37.5)	
Others	4 (66.7)	2 (33.3)	
Estrogen receptor			
Positive	112 (69.6)	49 (30.4)	0.24
Negative	21 (80.8)	5 (19.2)	
Progesterone receptor			
Positive	110 (69.2)	49 (30.8)	0.16
Negative	23 (82.1)	5 (17.9)	
HER2			
Positive	20 (62.5)	12 (37.5)	0.23
Negative	113 (72.9)	42 (27.1)	

[a] BMI: low, <23.3 kg/m^2; high, ≥23.3 kg/m^2

[b] *IDC* invasive ductal carcinoma, *ILC* invasive lobular carcinoma

ER, PR, and Ki67 expression levels in tumors of patients with high BMI

Findings of the analysis of ER expression levels by subtype of ER-positive breast cancers of patients in the two BMI groups are shown in Table 5. There were no significant differences between high and low BMI patients with luminal A and luminal B cancers, but ER expression of luminal/HER2 tumors of patients with high BMI [mean ± standard deviation (%), 90.4 ± 21.1] was significantly higher ($P = 0.001$) than that of patients with low BMI (40.5 ± 33.2). There were no differences in PR expression levels between the two BMI groups for any of the subtypes (Table 6). Because luminal A and luminal B breast cancers were initially classified according to the Ki67 expression level, we also classified luminal subtype (luminal A and luminal B), and their Ki67 expression levels were analyzed in relationship to high or low BMI (Table 7). However, there were no significant differences of Ki67 expression levels between the two BMI groups for any of the subtypes.

Table 3 Relationship between body mass index (BMI) and clinicopathological characteristics in postmenopausal patients

Characteristics	Low BMI[a] (%)	High BMI[a] (%)	*P* value
Tumor size			
≤2.0 cm	102 (53.4)	89 (46.6)	0.57
<2.0 cm	83 (56.5)	64 (43.5)	
Lymph node metastasis			
Negative	130 (54.4)	109 (45.6)	0.84
Positive	55 (55.6)	44 (44.4)	
Nuclear grade			
1	103 (45.5)	86 (54.5)	0.32
2	40 (39.4)	26 (60.6)	
3	36 (52.0)	39 (48.0)	
Unknown	6 (75.0)	2 (25.0)	
Histological type[b]			
IDC	174 (54.7)	144 (45.3)	0.55
ILC	5 (71.4)	2 (28.6)	
Others	6 (46.2)	7 (53.8)	
Estrogen receptor			
Positive	140 (52.6)	126 (47.4)	0.13
Negative	45 (62.5)	27 (37.5)	
Progesterone receptor			
Positive	116 (51.1)	111 (48.9)	0.05
Negative	69 (62.2)	42 (37.8)	
HER2			
Positive	27 (60.0)	18 (40.0)	0.44
Negative	158 (53.9)	135 (46.1)	

[a] BMI: low, <23.3 kg/m^2; high, ≥23.3 kg/m^2

[b] *IDC* invasive ductal carcinoma, *ILC* invasive lobular carcinoma

Discussion

The results of our study confirmed that higher BMI of premenopausal patients was significantly associated with lymph node metastasis and marginally associated with large tumor size as well as high nuclear grade. However, no such differences were detected in postmenopausal patients. In addition, we could not find any associations between BMI and breast cancer subtypes. Biglia et al. [11] found that postmenopausal patients with higher BMI (>25) showed a higher frequency of ER/PR-positive cancers than did those with lower BMI (87 % vs. 75 %), but no such difference was seen in premenopausal patients. Consistent with this observation, we found that the frequency of PR-positive tumors was marginally higher for postmenopausal patients but not for premenopausal patients with high BMI, which strongly suggests that a higher BMI influences tumor biology mediated through an increase in the production of estrogens.

Although high BMI was significantly more prevalent among postmenopausal (55.4 %) than premenopausal patients (30.3 %), the distribution of the subtypes was not significantly different for patients with either high or low BMI even when menopausal status was taken into consideration. Because ER, PR, and Ki67 expression levels of the subtypes did not differ between high and low BMI, except for ER expression levels in postmenopausal luminal/HER2 breast cancers, we hypothesize that the influence of high BMI on the biological characteristics of these tumor is limited. Alternatively, we confirmed that higher BMI was significantly associated with lymph node metastasis in premenopausal patients.

It has been reported that BMI of postmenopausal and/or premenopausal women is significantly associated with characteristics of the aggressive tumor phenotype, i.e., large tumor size, lymph node metastasis, and higher

Table 4 Relationship between body mass index (BMI) and breast cancer subtypes

Subtype	Low BMI[a]	High BMI[a]	*P* value
Premenopausal (*n*, %)			
Luminal A	63 (70.8)	26 (29.2)	0.34
Luminal B	38 (71.7)	15 (28.3)	
Luminal/HER2	11 (57.9)	8 (42.1)	
HER2	9 (69.2)	4 (30.8)	
TN	12 (92.3)	1 (7.7)	
Postmenopausal (*n*, %)			
Luminal A	69 (46.6)	79 (53.4)	0.12
Luminal B	59 (60.8)	38 (39.2)	
Luminal/HER2	12 (57.1)	9 (42.9)	
HER2	15 (62.5)	9 (37.5)	
TN	30 (62.5)	18 (37.5)	

Definitions of breast cancer subtypes are given in the "Materials and methods" section

[a] BMI: low, <23.3 kg/m^2; high, ≥23.3 kg/m^2

Table 5 Estrogen receptor (ER) expression levels by body mass index (BMI) in ER-positive subsets

Subtype	Low BMI[a]		High BMI[a]		*P* value
Premenopausal					
Luminal A	63	73.9 ± 23.8	26	73.6 ± 23.9	0.88
Luminal B	38	72.1 ± 26.4	15	79.9 ± 15.0	0.5
Luminal/HER2	11	53.3 ± 34.4	8	54.4 ± 39.5	0.71
Postmenopausal					
Luminal A	69	88.2 ± 14.9	79	83.1 ± 19.8	0.06
Luminal B	59	71.2 ± 36.4	38	76.0 ± 30.4	0.74
Luminal/HER2	12	40.5 ± 33.2	9	90.4 ± 21.1	0.001

Definitions of breast cancer subtypes are given in the "Materials and methods" section

[a] BMI: low, <23.3 kg/m^2; high, ≥23.3 kg/m^2; *n*, mean ± standard deviation (%)